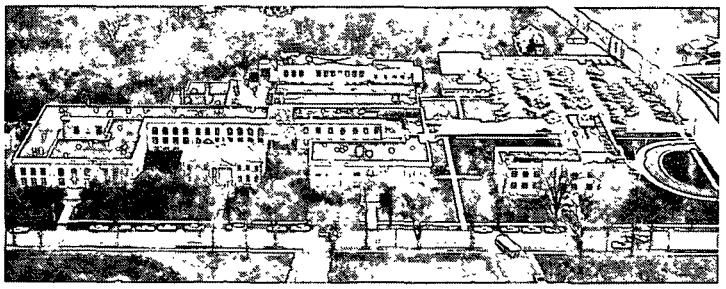

THE INSTITUTE OF PAPER CHEMISTRY, APPLETON, WISCONSIN

IPC TECHNICAL PAPER SERIES
NUMBER 271

MIPPS: A NUMERICAL MOVING BOUNDARY MODEL FOR IMPULSE DRYING

J. D. LINDSAY AND C. H. SPRAGUE

JANUARY, 1988

MIPPS: A Numerical Moving Boundary Model for Impulse Drying

J. D. Lindsay and C. H. Sprague

This manuscript is based on results obtained in IPC Project 3480 and is to be presented at the 1988 Annual Meeting of the Technical Section of CPPA in Montreal on January 26-29

MIPPS: A NUMERICAL MOVING BOUNDARY MODEL FOR IMPULSE DRYING

J. D. LINDSAY AND C. H. SPRAGUE

THE INSTITUTE OF PAPER CHEMISTRY
APPLETON, WISCONSIN 54912

ABSTRACT

A numerical moving boundary model has been developed to examine transient heat transfer and vapor-liquid displacement in impulse drying. The model, MIPPS, uses implicit, finite-difference forms of the mass, momentum, and energy conservation equations adapted for porous media. Predictions of water displacement, heat flux, and vapor pressure generation appear to be reasonable in light of available experimental data. While further work is needed, MIPPS represents a step toward understanding and improving innovative dewatering techniques for paper.

INTRODUCTION

Impulse drying is a novel process being developed at The Institute of Paper Chemistry which employs phase-change heat transfer. The process combines simultaneous application of intense heat and pressure to a wet paper web. Liquid water is removed from the paper rapidly and economically. The process not only offers significant energy and capital savings, but can give significantly improved paper properties (1).

Experimental work indicates that the key to impulse drying is the creation of a vapor phase within the sheet itself (1-3). The wet paper web (15-40% solids) is brought into a nip between two rolls, one of which is heated to 250-375 C. Nip pressure ranges from 3-6 MPa, and nip residence time is on the order of 20-100 milliseconds. While in the nip, vapor forms in the sheet next to the hot surface. Large hydraulic pressures are formed which resist the mechanically applied pressure, thus decreasing the densification of the sheet. The hydraulic pressure gradient helps drive liquid water out of the sheet into the felt below. The result is a sheet which is remarkably dry and has improved bulk properties in many cases.

The use of a gas phase to displace water in paper is an important dewatering mechanism not only in impulse drying, but also in through-drying and in other possible dewatering processes. To better understand the heat transfer and fluid flow mechanisms in impulse drying and other displacement processes, a numerical model has been developed. The model, MIPPS (Moving Interface Problems in Porous Systems), describes transient heat and fluid flow in vapor and liquid phases coupled with a moving boundary in a one-dimensional porous system. It is limited by a number of simplifications, but has already been of use in understanding the importance of heat transfer mechanisms in the impulse drying event. Specifically, a heat-pipe mechanism in which liquid water is resupplied to the heated surface of the paper is necessary to explain experimental results.

IMPULSE DRYING AS A MOVING BOUNDARY PROBLEM

Phase-change problems in which the phase boundary moves have received much attention recently. This class of moving boundary problems requires unique and difficult solution methods [see (4) for a review]. Analytical solutions are available only for the simplest cases, and are impossible when physical properties change with temperature. Such problems occur in many diverse areas, including ablation of heat shields in spacecraft, melting of permafrost, and the melting and solidification of alloys [several examples are treated in (5)]. In impulse drying, the vapor-liquid boundary moves not only because of phase change but also because the liquid is driven out by the generated vapor pressure. Impulse drying is thus related to another set of moving boundary problems involving phase displacement in porous media. The petroleum industry has been especially interested in such problems (6-7). Brownstock washing and air-through drying of paper are related displacement processes in the paper industry.

The combination of pressure-driven displacement and phase-change heat transfer makes the impulse drying process an unusual and especially complex moving boundary problem. Further complications come from the temperature-dependent physical properties of water and steam, from capillary effects, and from the compressible nature of the vapor phase (incompressibility has generally been assumed for both phases in past studies). Furthermore, contrary to the assumption made in virtually all past studies of moving boundary problems with phase change, the interface pressure and temperature are not constant but vary significantly with time.

In general, moving boundary problems require the simultaneous numerical solution of transport equations in two distinct phases which are coupled through boundary conditions at the moving phase boundary. The location of the interface is not known a priori, so iterative procedures are usually required. Both finite element and finite difference techniques have been used. One-dimensional problems are most commonly treated, although many recent studies have been published with two and even three-dimensional solutions (8-9).

A previous attempt at modeling the impulse drying process can be found in a thesis by Pounder (10). Pounder began with an elegant two-zone model of displacement from Ahrens (11), and aggressively extended it in order to model the entire, nonidealized impulse drying process with an explicit finite-difference method. He avoided a moving boundary approach, using an intuitive four-zone model instead. The derived equations, while complex, do not account for a number of important transient effects. The approach also appears to be too ambitious, making interpretation and analysis of predictions difficult. Although the pioneering work of Pounder has furthered understanding of the impulse drying process, it is felt that a true moving boundary approach with a more idealized system is needed to properly examine and understand the role of vapor pressure generation and phase change heat transfer in both impulse drying and in other displacement dewatering processes. MIPPS therefore represents a fundamental departure from Pounder's approach.

MODEL DEVELOPMENT

Model Assumptions and Equations. The porous medium is assumed to be rigid, isotropic, and homogeneous. The medium is assumed to be initially saturated with water, and then instantly brought into contact with a hot surface at temperature T_o. As heat flows into the liquid, a vapor phase forms which forces the free saturated liquid into the felt below (see Figure 1).

The vapor-liquid interface is assumed to be sharp. The effect of varying saturation and water inside the fibers is ignored at this stage, although capillary effects are considered (see discussion below). The two phases are joined through boundary conditions that apply only at the interface. Conservation equations for heat, mass, and momentum are applied simultaneously to both phases in such a way that the changing boundary conditions at the interface are constantly satisfied.

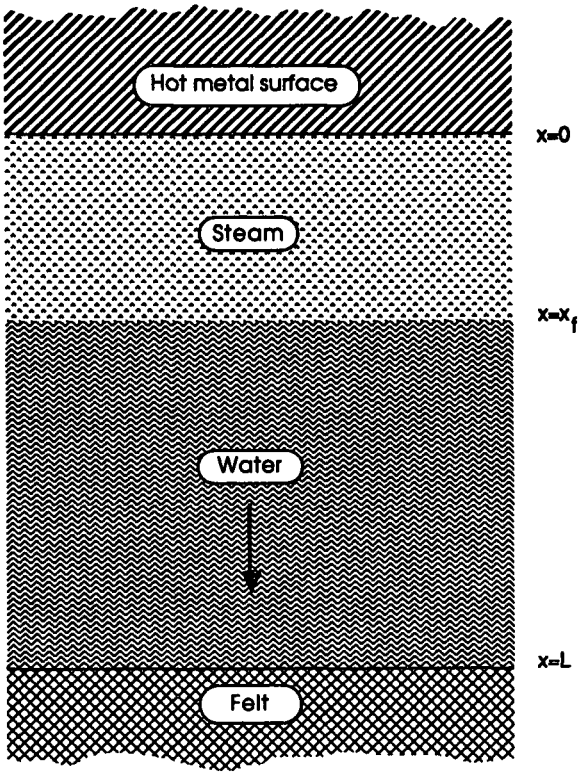

Figure 1. Displacement in paper during impulse drying.

The complexity of porous structures at the microscopic level prohibits the use of the standard microscopic transport equations. Volume averaging is required, but the results require empirical evaluation of constants such as permeability, and some uncertainty still exists over the correct forms of the transport equations (12). This is especially true for transient effects, for experimental confirmation of transport laws in porous media has been almost exclusively limited to steady-state processes. In spite of uncertainties, forms of the transport equations have been chosen which should be appropriate for the current problem. The physical properties in these equations are temperature dependent.

The proper form of the continuity equation for the gas phase is

$$\varepsilon\frac{\partial \rho}{\partial t}+\frac{\partial(\rho u)}{\partial x}=\dot{m} \qquad (1)$$

where ε is the porosity, ρ is the density, u is the superficial velocity (volumetric flow rate divided by area), and $\dot{m}$ is the local volume-averaged rate of evaporation in kg/sm^2 [adapted from (13), p. 150].

The transient momentum equation for the compressible gas phase is based on the Navier-Stokes equations incorporating Darcy's law with

extensions from Brinkman and Forchheimer [adapted from (14)]:

$$\frac{\rho}{\varepsilon}\left(\frac{\partial u}{\partial t}+u\frac{\partial u}{\partial x}\right)=-\frac{\partial P}{\partial x}+\frac{1}{\varepsilon}\frac{\partial}{\partial x}\left(\mu\frac{\partial u}{\partial x}\right)-\left(\frac{\mu_f}{K}+\frac{\rho C|u|}{\sqrt{K}}\right)u \qquad (2)$$

Here P is the pressure, μ is the vapor viscosity, K is the permeability, and C is an empirical constant. The term containing C (Forchheimer's correction) accounts for inertial effects, which are unlikely to be important at the low gas velocities involved in impulse drying. C has therefore been set to zero in the current version of MIPPS.

The energy equation for the gas phase must account for the compressible nature of steam; the gas phase is not divergence-free. Equation 10.1.19 from Bird et al. (13) is adapted to porous media. The ideal gas law is assumed, and viscous dissipation terms are ignored, resulting in

$$\rho C_v\left(\frac{\partial T}{\partial t}+u\frac{\partial T}{\partial x}\right)=\frac{-\partial}{\partial x}\left(k\frac{\partial T}{\partial x}\right)-\frac{P\,\partial u}{\varepsilon\,\partial x}+\dot{m}h_v \qquad (3)$$

where C_v is the constant-volume heat capacity, k is the thermal conductivity, P is the pressure, and h_v is the heat of vaporization. Because cellulose has a significantly lower thermal diffusivity than steam, the effect of the solid matrix on heat conduction has been ignored at this stage. This assumption will be inaccurate for low-porosity media. Properly accounting for the effect of the solid phase would modify the values of the physical properties in Eq. (3) (12,15). Vaporization is assumed to occur at boundaries in the current version of MIPPS, so the last term in Eq. (3) is not applicable to most of the flow.

The liquid phase is assumed to be incompressible, giving $\partial u/\partial x = 0$. Heat transfer in the liquid phase is given by

$$\rho C_p\left(\frac{\partial T}{\partial t}+u\frac{\partial T}{\partial x}\right)=\frac{-\partial}{\partial x}\left(k\frac{\partial T}{\partial x}\right) \qquad (4)$$

where C_p is the constant-pressure heat capacity.

The transient liquid velocity is given by the momentum transport equation modified for incompressible flow in porous media:

$$\frac{\rho\,\partial u}{\varepsilon\,\partial t}=\frac{-\partial P}{\partial x}-\frac{\mu u}{K\rho}+\rho g \qquad (5)$$

where g is the gravitational component in the direction of flow. By taking advantage of the continuity equation to convert the partial differential into an ordinary differential, a macroscopic equation for the liquid velocity is obtained:

$$\frac{1}{\varepsilon}\frac{du}{dt}=\frac{-1}{\rho}\frac{P_{int}-P_\infty}{L-x_f}-\frac{u}{K\rho}\frac{\int_{x_f}^{L}\mu(T(x))dx}{L-x_f} \qquad (6)$$

where L is the thickness of the porous medium (the sheet), x_f is the location of the interface, P_{int} is the pressure at the interface, and P_∞ is the specified pressure at the exit boundary of the system. Gravity has been neglected in this equation.

Boundary Conditions. At the top surface of the porous system, the temperature is specified. It can vary with time, but was held constant at 600°K (620°F) for the predictions reported in this paper. There is no mass flow at this boundary. At the outlet boundary (the paper-felt boundary), the effective thermal conductivity is set to zero. This boundary condition allows heat to be removed by convection but implicitly assumes that water entering the felt is no longer in thermal contact with water in the sheet. The liquid velocity at the outlet boundary is the same as the bulk liquid velocity. The pressure at this boundary is specified and constant. It has been set to atmospheric pressure in most of the MIPPS predictions made to date.

The gas and liquid phases are joined through boundary conditions at the interface. The interface is a common boundary between the two phases with a single temperature, velocity, and pressure. The temperature and pressure are required to be in equilibrium. The velocity is the liquid velocity plus a contribution from evaporation or condensation at the interface:

$$U_{int}=U_L+\frac{\dot{m}}{\rho} \qquad (7)$$

where U_{int} is the interface velocity and U_L is the bulk liquid velocity. The evaporation rate is determined by the difference between the incoming heat flux from the gas phase and the outgoing heat flux into the liquid phase:

$$\left(-k\frac{\partial T_G}{\partial x}\right)-\left(-k\frac{\partial T_L}{\partial x}\right)=\dot{m}\,h_v \qquad (8)$$

where the subscripts G and L refer to the gas and liquid phases, respectively.

Capillarity. Capillary forces in the porous system are accounted for, but in a simplistic way. Capillary effects cause a discontinuity in pressure at the vapor-liquid interface given by

$$P_g-P_l=\frac{2\sigma}{r_\theta}, \qquad (9)$$

where P_g is the gas pressure, P_l is the pressure of the liquid, and σ is the surface tension. The effective meniscus radius, r_e, is given by

$$\frac{2}{r_e} = \frac{1}{r_1} + \frac{1}{r_2} \qquad (10)$$

where r_1 and r_2 are the principal radii of curvature. The curved interface also affects the equilibrium condition of the vapor and liquid. The equilibrium pressure of the liquid at a given temperature can be found iteratively with the relationship (16):

$$P_o - P_l = \frac{\rho_l RT}{M} \ln \frac{P_o}{P_l + \frac{2\sigma}{r_e}} \qquad (11)$$

where P_o is the saturation pressure of the liquid in a large volume (i.e., with a flat meniscus). The porous medium changes the equilibrium states of the liquid and vapor so that both are superheated.

The limitation in the treatment of capillary forces comes in the assumption that a sharp interface separates the vapor region from the liquid region. In reality, a region of variable saturation should exist which would allow water to be wicked back toward the surface. It has been hypothesized that the resupply of water to the hot surface via capillary wicking helps sustain the high rates of heat transfer observed in impulse drying. To examine this hypothesis, MIPPS allows the user to specify a rate of water resupply (or wicking rate) from the saturated zone to a location near the hot surface. The resupplied water then undergoes phase change. While this approach is oversimplified, it does allow some wicking effects to be examined. This simplistic treatment is tantamount to assuming that the porous medium consists of two sets of parallel cylindrical tubes initially filled with water. One set has radii small enough for capillary forces to wick water to the surface against the gas pressure gradient, whereas the pressure gradient causes liquid displacement in the other set of tubes with larger radii.

Numerical Solution. The transport equations are discretized into finite difference equations. Convective terms (such as $u\partial T/\partial x$) use backward differencing (i.e., upwind differencing with the assumption of flow toward the felt), while central differencing is used for other terms. The methods outlined by Patankar (17) were used for most of the numerical development. The resulting simultaneous equations form a tridiagonal matrix which is solved using the Crout reduction algorithm (18).

A staggered grid approach is used with pressure nodes between the velocity and temperature nodes as shown in Figure 2. Nodes for pressure, velocity, and temperature exist at the interface. The grids are nonuniform, with grid spacing becoming increasingly dense near the interface. The number of nodes assigned to each phase is allowed to vary as the interface moves. This feature maintains a common level of accuracy as the interface moves, but again increases the complexity of the code. The grids also move as the interface moves in order to constantly keep a node at the interface. Moving grids in a transient process require that information from the previous time step be transferred to the new grid structure to be used during the current time step. Furthermore, since the location of the interface is not known until convergence within a time step has been achieved, the interface location must be guessed and iterated upon, with grid restructuring required at each iteration. The user can specify either linear or cubic spline interpolation to transfer information to new grid structures between and during time steps. The MIPPS cases reported here used linear interpolation to conserve computer time.

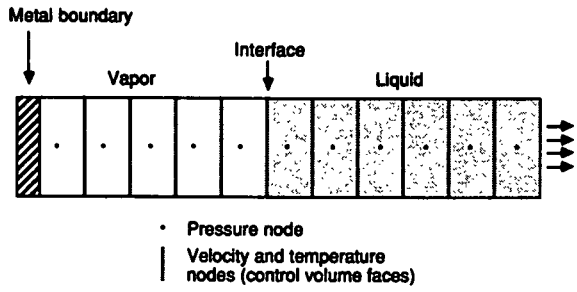

Figure 2. Schematic of MIPPS node structure. Nodes are not uniformly spaced but become increasingly dense near the interface. Usually 50-100 nodes are used.

Significant complications stem from the changing gas pressures and interface equilibrium conditions. Underrelaxation and iteration of interface boundary conditions during the solution for each time step are required.

The compressible gas phase also increases the complexity of the code. A compressible form of the popular SIMPLE pressure correction scheme was derived using principles outlined in Patankar (17). Attempts to use the standard SIMPLE procedure consistently resulted in divergence. The SIMPLE approach begins with an assumed pressure field, P*. This pressure field is used to solve for the velocity and temperature fields. These resulting solutions can be

used to obtain a pressure correction field, P', which, when added to P*, yields a new pressure field that satisfies the continuity equation. The corrected pressure field (P' + P*) now becomes the new assumed field, P*, and the process iterates until the correction terms, P', become small. This approach guarantees that the solutions to the momentum and energy equations are compatible with the continuity equation.

The size of the time steps is not constant, but increases slightly after each iteration. As the interface velocity increases, however, the time step may be automatically reduced. The time step must always be small enough to prevent the interface from advancing more than the spacing of one node at a time.

The procedure in obtaining a solution at any time step consists of the following steps:

1. Estimate the new interface location and the evaporation rate at the interface. ("New" refers to the new conditions which will exist at the end of the current time step.)
2. Restructure the grids, keeping nodes at the interface and redistributing the nodes between gas and liquid phases as needed.
3. Use the previous gas-phase pressure field as the present assumed pressure field, P*.
4. Using P*, solve for the gas-phase temperature and velocity fields.
5. Solve for the pressure corrections, P', necessary to solve the continuity equation. Pressure corrections are used to correct the pressure, velocity and temperature fields.
6. The corrected pressure field becomes P*. If P' is small, go to the next step. Otherwise return to step 4.
7. Adjust the interface temperature toward the equilibrium value.
8. Solve for the liquid temperature field and the liquid velocity.
9. Use the computed heat fluxes in and out of the interface to obtain the current vaporization rate (can be positive or negative) and interface velocity.
10. Go to step 3 and continue until equilibrium at the interface exists.
11. If the residuals for the continuity, momentum, and energy equations are small, go to the next step. Otherwise go to step 1 and repeat.
12. Convergence has been achieved. Advance the time step, store the results, and go to step 1.

Once MIPPS was written, several test cases were run to examine the accuracy of the model. For instance, the boundary conditions and initial conditions were altered in the code to create a sealed, insulated porous system with a gas phase and a liquid phase that were not in equilibrium. MIPPS then computed the transient behavior of the system as the vapor and liquid approached equilibrium. The steady state conditions could be determined a priori from thermodynamic considerations. After several hundred time steps, the computed system temperature, pressure, and vapor/liquid distribution were examined. Within the limits of rounding error in the output results, the computed pseudo-equilibrium values agreed with the thermodynamic prediction. This was a crude test and does not prove the code is correct in any sense, but is an encouraging indication; more sensitive checks of thermodynamic soundness are still needed. Other simple tests for physical reasonableness were conducted at each stage of model development, and the code appears to be reasonable.

MIPPS is general enough that it can be applied to processes other than impulse drying. Boundary conditions need to be altered for each new physical arrangement, and some subroutines may need to be turned off. In addition, subroutines for some special physical processes may need to be added.

MIPPS RESULTS

Predictions for impulse drying-like situations have been made. The MIPPS predictions were obtained using either a VAX 11/780 or a Macintosh Plus with an accelerator board and a math coprocessor (the latter is almost as fast as the VAX). Convergence times on the Macintosh usually ranged from 0.5 to 10 CPU seconds per time step, depending on the size of the time step and the details of the case. While 50 total computational nodes across the paper was the norm, some predictions were made with 80 or 100 nodes.

The cases reported here were computed using an initial liquid temperature of 100°C, a constant surface temperature of 327°C, a sheet thickness of 1.0 mm, and an ambient pressure of 1.013×10^5 Pa (1 atm). An effective pore radius of 5 μm was also assumed in the treatment of capillarity. A highly porous medium has been arbitrarily assumed with a porosity of unity (predictions with lower porosities are generally similar to those reported here, although only a few predictions have been made). Only permeability and water resupply rate were varied in the following predictions.

Interface Motion and Vapor Pressure. Figure 3 shows MIPPS predictions for two different permeabilities at a constant wicking rate of 0.5 kg/sm^2. In Figure 3a, an order of magnitude change in permeability changes the magnitude of the peak gas pressure by a factor of about 2.5, a result which is consistent with other predic-

tions. In Figure 3b, 60% of the free water is displaced within 50 milliseconds when the paper has a permeability of 1.0×10^{-15} m^2. Displacement is about 4 times as rapid when the permeability is increased by a factor of 10. These rates are consistent with observed dewatering rates in impulse drying of linerboard, for which the permeability under compression should be on the order of 10^{-14} to 10^{-15} m^2. Examination of Figures 3a and 3b shows that when the permeability is lower, the increasing vapor pressure gets less 'relief' from the moving liquid seal and thus higher pressures are achieved. The higher pressure means a greater force for liquid removal, which partially compensates for the increased resistance to flow.

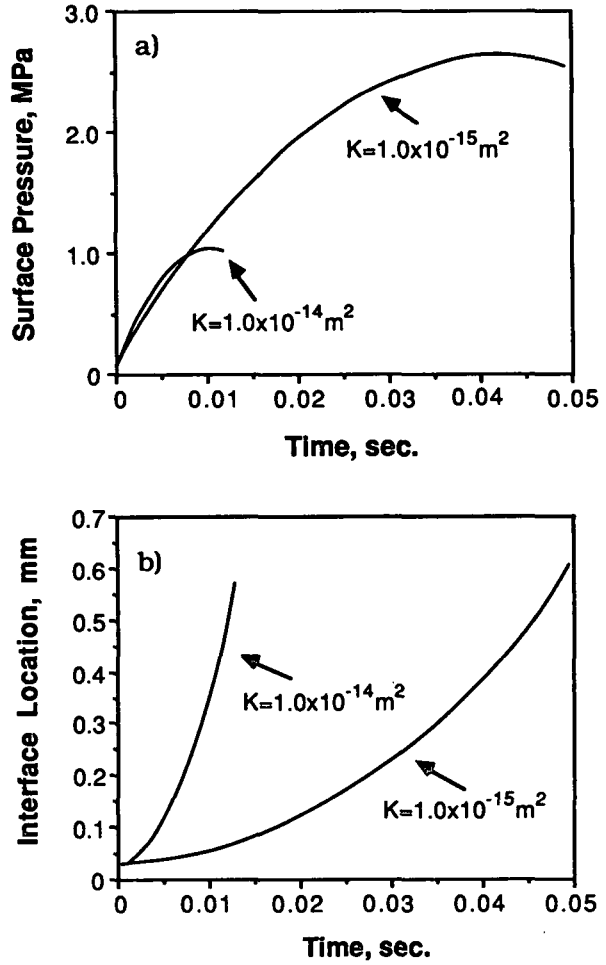

Figure 3. Effect of permeability on gas-phase pressure development and on vapor-liquid interface location. For both cases, surface temperature was set to 600°K, ambient pressure was 101.3 kPa, reflux ratio was 0.5 kg/sm^2, and the effective pore radius was 5 µm.

Burton (2) attempted to measure vapor pressures in the sheet during impulse drying, and reported peak pressures on the order of 0.7 MPa in linerboard. Predicted vapor pressures from MIPPS have ranged from 0.04 to 4 MPa for permeabilities of 10^{-13} to 10^{-15} m^2 and wicking rates of 0 to 1.0 kg/sm^2. Burton's results cannot be properly compared to any single MIPPS prediction at this time, but his pressure measurements seem to be consistent with MIPPS and may be of use in evaluating more comprehensive versions of MIPPS in the future. Burton's results also indicate an approximate square-root-of-time dependence for vapor pressure, which is also consistent with MIPPS predictions.

The predictions of interface movement in Figure 4 show a strong dependence on wicking rate. A permeability of 1.0×10^{-15} m^2 was assumed, with wicking rates of 0.5 and 1.0 kg/sm^2. The effect of wicking becomes more pronounced with time. Wicking greatly increases the rate of dewatering because it increases the evaporation rate and allows higher gas-phase pressure to develop.

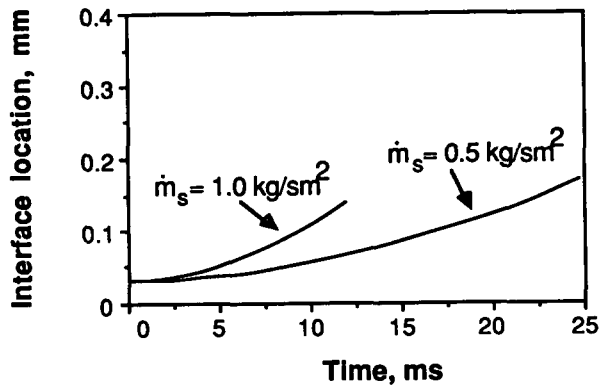

Figure 4. Effect of water resupply rate to surface on interface motion in MIPPS predictions. Permeability was 1.0×10^{-15} m^2, surface temperature was 600°K; and the effective pore radius was 5.0 µm.

Transient Heat Flux. MIPPS predictions of the transient heat flux rate show that significant wicking is required to explain the experimentally observed heat fluxes in impulse drying, which are on the order of $1\text{-}3 \times 10^6$ W/m^2. Conduction heating through the vapor phase plays an important role, but continued boiling at the surface of the resupplied water must also be occurring in impulse drying. Figure 5 compares two MIPPS predictions with experimental heat flux data from Burton. The predictions are applied to the portion of the impulse drying event in which little compression of the paper occurs (i.e., where the assumption of a rigid porous medium is appropriate). Again, comparisons of Burton's impulse drying data with MIPPS predictions must be viewed cautiously because MIPPS does not simulate the full impulse drying event. The physical properties of Burton's linerboard are also not known accurately, although a permeability of 10^{-15} m^2 should

be reasonable. Two values of wicking rate were used, one of which (1.0 kg/sm^2) gives results that agree favorably with a portion of the experimental data. Based on a number of predictions, however, it does appear that wicking rates on the order of 1.0 kg/sm^2 are needed to account for the measured rates of heat transfer. This wicking rate can easily be provided by capillary forces. For instance, if water at 210°C (400°F) is resupplied to the surface across a 200 μm zone through pores 1 μm in diameter, less than 1% of the surface area of the sheet must be occupied by such pores to provide 1 kg/sm^2 of water to the surface, assuming a negligible gas-phase pressure gradient.

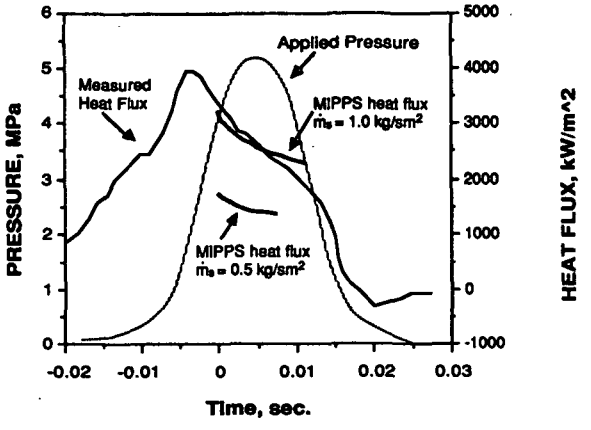

Figure 5. Comparison of experimental heat flux data from Burton (12) with two MIPPS predictions. MIPPS predictions assumed K = 1.0 x 10^{-15} m^2, effective pore radius = 5.0 μm, and surface temperature = 600°K (327°C or 620°F). Water resupply rate was varied from 0.5 to 1.0 kg/sm^2.

Water resupply rates are apparently limited by boiling heat transfer mechanisms, for the observed heat transfer rates are close to the steady-state critical boiling levels. The details of such mechanisms are the topic of current doctoral research by Gary Rudemiller at The Institute of Paper Chemistry.

SUMMARY

The compressibility of the gas phase and the combination of phase change and porous displacement make MIPPS a unique thermal moving boundary model. MIPPS is still highly idealized and represents only one step in a long-term effort to understand and improve the impulse drying process and other displacement strategies. Much work remains to be done in validating and applying the model, but it has already clarified the importance of capillary wicking in impulse drying. Wicking not only accounts for the observed high rates of heat transfer in impulse drying, but also leads to increased vapor pressures that drive the liquid water out of the sheet more rapidly. MIPPS predictions also appear to be consistent, at least qualitatively, with a number of measurements in impulse drying events.

Future plans include extending MIPPS to deformable porous media. A more sophisticated approach is also under development to more properly account for variable saturation. A number of minor areas need improvement, including treatment of solid-phase conduction, nonuniform permeability and porosity, and bound water in the fibers. Pounder (1986) employed many physical property relationships in his model which will be of value in future MIPPS developments.

REFERENCES

1. LAVERY, H., Project 3470 Status Report to the Engineering Project Advisory Committee, The Institute of Paper Chemistry, Appleton, Wisconsin (Oct. 22, 1987).
2. BURTON, S. W. An Investigation of Z-direction Density Profile Development During Impulse Drying. Ph.D. Thesis, The Institute of Paper Chemistry (June, 1986).
3. BURTON, S. W., and SPRAGUE, C. H. The Instantaneous Measurement of Density Profile Development During Web Consolidation. J. Pulp Paper Science 13(5):J145-J149 (1987).
4. CRANK, J. How to Deal with Moving Boundaries in Thermal Problems. Numerical Methods in Heat Transfer. Ed., Lewis, R. W., Morgan, K., and Zienkiewicz, O. C. New York: John Wiley and Sons (1981).
5. OCKENDON, J. R., and HODGKINS, W. R., editors. Moving Boundary Problems in Heat Flow and Diffusion. Oxford: Clarendon Press (1975).
6. HOMSY, G. M. Viscous Fingering in Porous Media. Ann. Rev. Fluid Mechanics 19:271-311(1987).
7. GORELL, S. B. and HOMSY, G. M. A Theory for Most Stable Variable Viscosity Profile in Graded Mobility Displacement Processes. AIChE J. 31(9):1498-1503(1985).
8. HASTAOGLU, M. A. Numerical Solution of Three-Dimensional Moving Boundary Problems: Melting and Solidification with Blanketing of a Third Layer. Chem. Eng. Sci. 42(10): 2417-2421(1987).
9. MORGAN, K., LEWIS, R. W., and ROBERTS, P. M. Solution of Two-Phase Flow Problems in Porous Media via an Alternating-direction Finite Element Method. App. Math. Modeling 8:391-396(1984).

10. POUNDER, J. R. A Mathematical Model of High Intensity Paper Drying. Ph.D. Thesis, The Institute of Paper Chemistry, Appleton, Wisconsin (Jan., 1986).

11. AHRENS, F. Wet Pressing Fundamentals. Project 3480 Status Report, The Institute of Paper Chemistry, Appleton, Wisconsin (Sept. 1984).

12. GREENKORN, R. A. Steady Flow through Porous Media. AIChE J. 27(4):529-545 (1981).

13. BIRD, R. B., STEWART, W. E., and LIGHTFOOT, E. N. Transport Phenomena, New York, John Wiley and Sons (1960).

14. BECKERMAN, C., RAMADHYANI, S., and VISKANTA, R. Natural Convection Flow and Heat Transfer Between a Fluid Layer and a Porous Layer Inside a Rectangular Enclosure. J. Heat Transfer 109(2):363-370 (1987).

15. REDDY, G. B., and MULLIGAN, J. C. Macroscopic Continuum Analysis of Simultaneous Heat and Mass Transfer in Unsaturated Porous Materials Containing a Heat Source. Int. Comm. Heat Mass Transfer 14(3):251-263(1987).

16. UDELL, K. S. Heat Transfer in Porous Media Heated from Above with Evaporation, Condensation, and Capillary Effects. J. Heat Transfer 105(3):485-492(1983).

17. PATANKAR, S. V. Numerical Heat Transfer and Fluid Flow. Washington, D.C., Hemisphere Publishing Corp. (1980).

18. BURDEN, R. L., FAIRES, J. D., and REYNOLDS, A. C. Numerical Analysis. Boston, Prindle, Weber, and Schmidt (1981).